

Contact Properties of Pt/RuO₂/Ru Electrode Structure Integrated on Polycrystalline Silicon

Eun-Suck Choi, Jun-Sik Hwang, and Soon-Gil Yoon*^z

Department of Materials Engineering, Chungnam National University, Taejeon 305-764, Korea

The buffer layers of RuO₂/Ru in Pt/RuO₂/Ru/poly-Si (polycrystalline silicon) structure were prepared by metallorganic chemical vapor deposition (MOCVD) and dc magnetron sputtering. The barrier layers of RuO₂/Ru deposited by MOCVD showed a stable interface, and did not affect the surface morphology of the platinum bottom electrode even at a high annealing temperature of 800°C. The barrier layers effectively prevented the interdiffusion of Pt, O, and Si at annealing temperatures above 700°C in O₂ ambient. On the other hand, the barrier layers of RuO₂/Ru formed by dc sputtering showed severe intermixing and strongly influenced the platinum morphology at high temperature annealing. Contacts in Pt/MOCVD(RuO₂/Ru)/poly-Si and Pt/dc sputtered (RuO₂/Ru)/poly-Si structures showed the specific contact resistance of 5.0×10^{-5} and $2.0 \times 10^{-3} \Omega \text{ cm}^2$, respectively. The barrier layers of RuO₂/Ru formed by MOCVD in Pt/RuO₂/Ru/poly-Si structure were attractive for integration of high dielectric constant (Ba,Sr)TiO₃.

© 2000 The Electrochemical Society. S0013-4651(99)11-088-7. All rights reserved.

Manuscript submitted November 24, 1999; revised manuscript received March 3, 2000.

Barium strontium titanate, (Ba,Sr)TiO₃ (BST), thin films have received a great deal of attention as a likely candidate for dynamic random access memory (DRAM) applications.¹⁻³ The integration of BST films into a DRAM capacitor structure has many problems. One of the primary problems is the need to deposit the BST films under oxidizing conditions and to minimize postdeposition thermal treatments under low oxygen partial pressures, as the perovskites are susceptible to reduction. This also limits the choice of electrodes for the capacitor stack to either Pt, Ru, or conducting oxides, since forming an insulating oxide at the BST-electrode interface will lower the stack capacitance. The choice of electrode materials is important for both processing and integration. The major developments in the bottom electrode contacts were performed by NEC,⁴ Mitsubishi,⁵ and earlier work by NEC.⁶ The electrode stack structures suggested by NEC, Mitsubishi, and earlier work by NEC were Al/TiN/BST/RuO₂/TiN/thin Ti/poly-Si plug, Ru/BST/Ru/poly-Si, and top electrode/BST/Pt/TiN/Ti/poly-Si, respectively. However, thus far, the suggested electrode structures have many problems for DRAM devices applications.

Generally, electrode structures for integration of the high dielectric materials onto polysilicon were fabricated by sputtering. However, the electrodes and the barrier layers formed by sputtering have large stress. When they are exposed to high temperature for deposition of high dielectric materials, hillocks are formed by the interdiffusion of elements to relieve the high stress, resulting in electrical failure to capacitors. However, because metallorganic chemical vapor deposition (MOCVD) was performed by the diffusion and the surface reaction of sources under the equilibrium state, MOCVD layers have a dense structure and low stress. Therefore, the electrode structures formed by MOCVD were expected to be able to alleviate the formation of hillocks and the intermixing of elements when they are exposed to high temperature in order to deposit the high dielectric materials. The evaluation of the electrode structures formed by MOCVD for integration of high dielectric thin films has not been reported elsewhere.

In this paper, we report the bottom electrode stack structures of Pt/RuO₂/Ru/poly-Si. The barrier layers of RuO₂/Ru on poly-Si were deposited by MOCVD and dc sputtering. Ruthenium barrier layer plays an important role in increasing the adhesion between Pt and poly-Si and in preventing the oxidation of poly-Si during the deposition of high dielectric materials. Ruthenium dioxide also plays role in preventing the diffusion of Ru through Pt grain boundary and then the formation of RuO_x phase on the platinum surface. RuO₂/Ru bar-

rier layers were also expected to block the interdiffusion of Pt and Si elements. The structural and the electrical properties of Pt/dc sputtered (RuO₂/Ru)/poly-Si and Pt/MOCVD (RuO₂/Ru)/poly-Si electrode structures were evaluated under more severe annealing conditions than under the deposition of BST by MOCVD.

The barrier layers of RuO₂/Ru were deposited onto poly-Si (200 nm)/SiO₂ (100 nm)/Si (001) substrates by MOCVD and dc sputtering, respectively. The native oxides on poly-Si were eliminated with the following schedule. Wafers were etched for 10 s using a 2.5% HF solution and then rinsed with deionized water for 5 min in ultrasonic cleaner. After rinsing, wafers were etched again for 5 s in a 6:1 HF solution buffered using C₂H₅OH. Finally, they were dried with nitrogen (99.9999% purity). The bottom electrodes of Pt were also prepared on RuO₂/Ru/poly-Si by MOCVD. The growth system of MOCVD used for the Ru, RuO₂, and Pt deposition consists of a vertical cold-wall reactor. The detailed deposition conditions by MOCVD and dc sputtering are summarized in Table I. Ruthenium dioxide by MOCVD was sequentially deposited on ruthenium in O₂ ambient after deposition of Ru on poly-Si without oxygen. The platinum electrodes and RuO₂/Ru barrier layers were deposited on poly-Si as a thickness of about 150 and 50 nm, respectively. The barrier layers are composed of 30 nm thick RuO₂ and 20 nm thick Ru. The residual stress existing at the films was measured by X-ray diffraction (XRD) using $\sin^2 \Phi$.^{7,8} The film thickness and the surface morphologies were determined from cross-sectional and surface images by scanning electron microscopy (SEM, AKASHI DS-130C). The depth-profile of electrode structures was determined by Auger electron spectroscopy (AES, VG Scientific Microlab 310-D). The resis-

Table I. Deposition conditions of Ru/RuO₂ by MOCVD and dc sputtering, and Pt films by MOCVD.

Deposition parameter	dc-sputtered (RuO ₂ /Ru)	MOCVD (RuO ₂ /Ru)	MOCVD-Pt
Source material	Ru metal target	Ru ₃ (CO) ₁₂	MeCpPtMe ₃ ^a
Deposition temperature	300°/400°C	250°C	400°C
Substrate	Poly-Si	Poly-Si	RuO ₂ /Ru/poly-Si
Ar gas flow rate	10 sccm	200 sccm	50 sccm
Bubbling temperature	—	110°C	10°C
Deposition pressure	1×10^{-2} Torr	2 Torr	0.5 Torr
Oxygen flow rate	10/0 sccm	50/0 sccm	50 sccm

^a (Trimethyl)methylcyclopentadienylplatinum {(CH₃)₃(CH₃C₅H₄)Pt}.

* Electrochemical Society Active Member.

^z E-mail: syoon2@unity.ncsr.edu

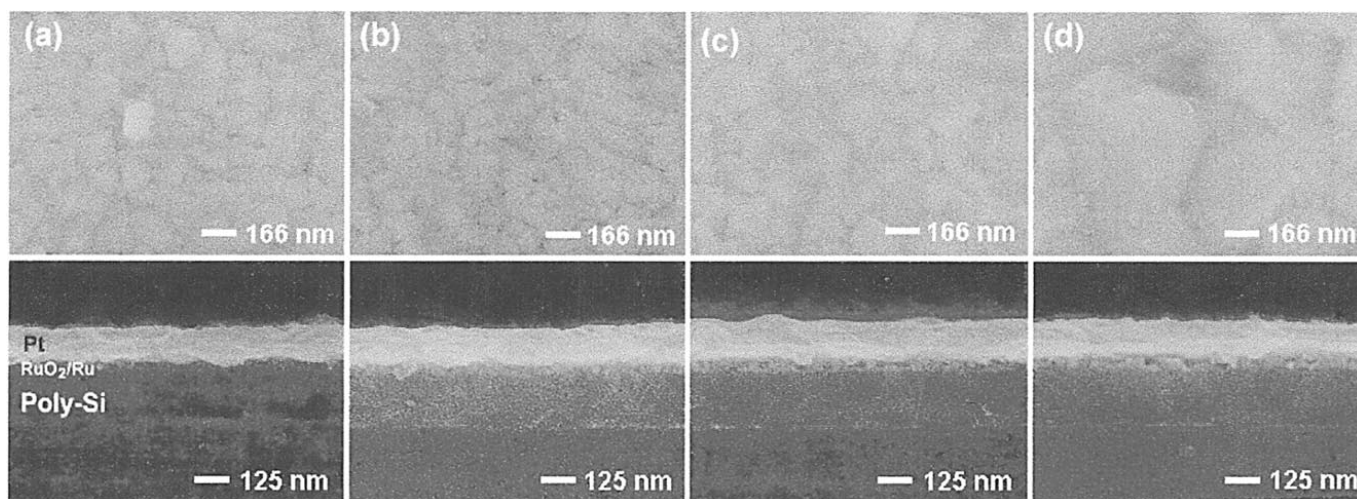


Figure 1. SEM surface and cross-sectional images of Pt/MOCVD (RuO_2/Ru)/poly-Si (a) as-deposited, and annealed at (b) 600, (c) 700, and (d) 800°C for 1 h in O_2 (760 Torr).

tivity of electrode structures was measured by electrometer (CMT-SR 1000) using a four-point probe. Current-voltage (I-V) characteristics were then measured using an HP 34401A multimeter and Keithley 224 programmable current source. The specific contact resistance of electrode structures was measured with the experimental configuration known as the transfer length method (TLM).⁹ The contact patterns were prepared by Ar-ion milling and photolithography. Ion milling is conducted at a tilt angle of 15° from the ion beam direction at 8×10^{-4} Torr with a 350 V argon ion beam. The photolithography is done with AZ5214E photoresist (PR).

Figure 1 shows SEM surface and cross-sectional images of Pt/ RuO_2/Ru /poly-Si electrode structures as-deposited by MOCVD and annealed at different temperatures in oxygen ambient (760 Torr). The barrier layers of RuO_2/Ru formed by MOCVD showed clear interfaces after annealing at sufficiently high temperature of 800°C. The platinum bottom electrodes also show the smooth and dense morphologies, and slight grain growth with increasing annealing temperature. These results suggested that the RuO_2/Ru layer formed by MOCVD did not affect the microstructure of Pt bottom electrode. Figure 2 shows SEM surface and cross-sectional images of Pt/ RuO_2/Ru /poly-Si electrode structures as-deposited by dc sputtering and annealed at different temperatures in oxygen ambient (760 Torr). The interface between platinum and RuO_2/Ru was not clear due to severe interdiffusion with increasing annealing temperature. Platinum sur-

face showed extremely rough morphology in samples annealed at 700°C. This result might be considered because ruthenium diffused through the Pt grain boundary was formed RuO_x second phase on the platinum surface during annealing in oxygen ambient. This behavior of ruthenium in electrode structure can be explained by residual stress of ruthenium. The residual stress of 20 nm thick ruthenium deposited on polysilicon was measured at room temperature using XRD peak of (101) existing at $2\theta = 42^\circ$. The dc-sputtered and MOCVD-Ru films have a compressive stress of about 2.1 and a tensile stress of about 0.05 GPA, respectively. When dc-sputtered ruthenium having a large compressive stress was annealed at high temperature of 700°C, ruthenium diffused to platinum surface through RuO_2 and platinum grain boundary to relieve the large compressive stress. Then ruthenium diffused to platinum surface forms the second phase on platinum surface during oxygen ambient annealing. Because RuO_2 layer formed by dc-sputtering is oxygen-poor compared with that by MOCVD, dc-sputtered RuO_2 layer is less effective than that of MOCVD- RuO_2 as a diffusion barrier of Ru. The platinum surface annealed at high temperature in oxygen ambient shows a rough morphology due to the formation of second phase. On the other hand, because MOCVD was performed by diffusion and the surface reaction of sources under the equilibrium state, deposition layers have a dense structure and a low tensile stress compared with sputtering method. Therefore, the electrode structures formed by MOCVD

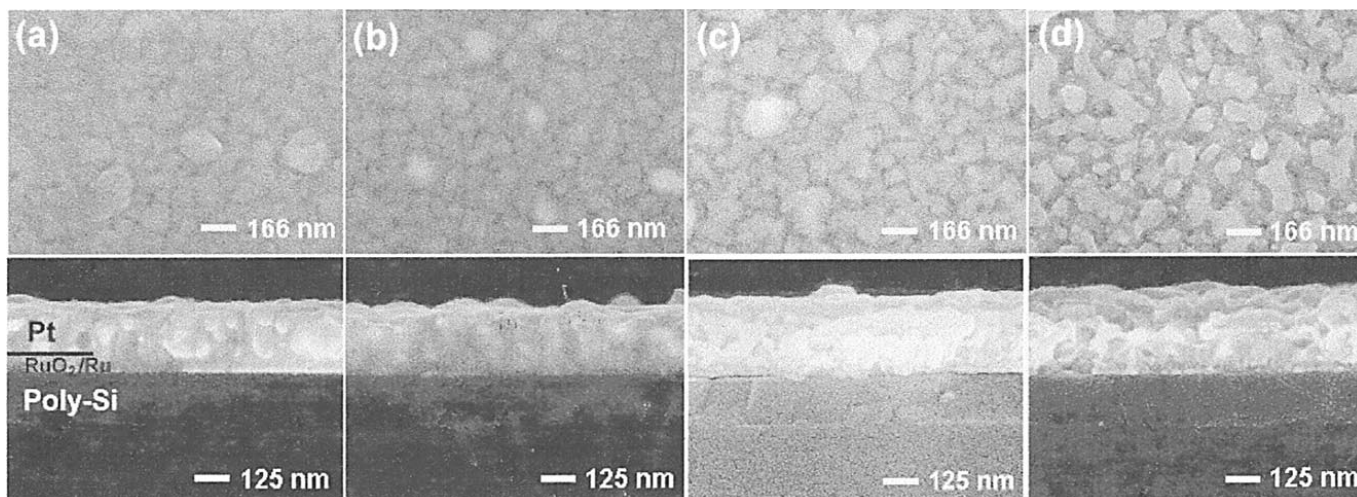


Figure 2. SEM surface and cross-sectional images of Pt/dc sputtered (RuO_2/Ru)/poly-Si (a) as-deposited, and annealed at (b) 500, (c) 600, and (d) 700°C for 1 h in O_2 (760 Torr).

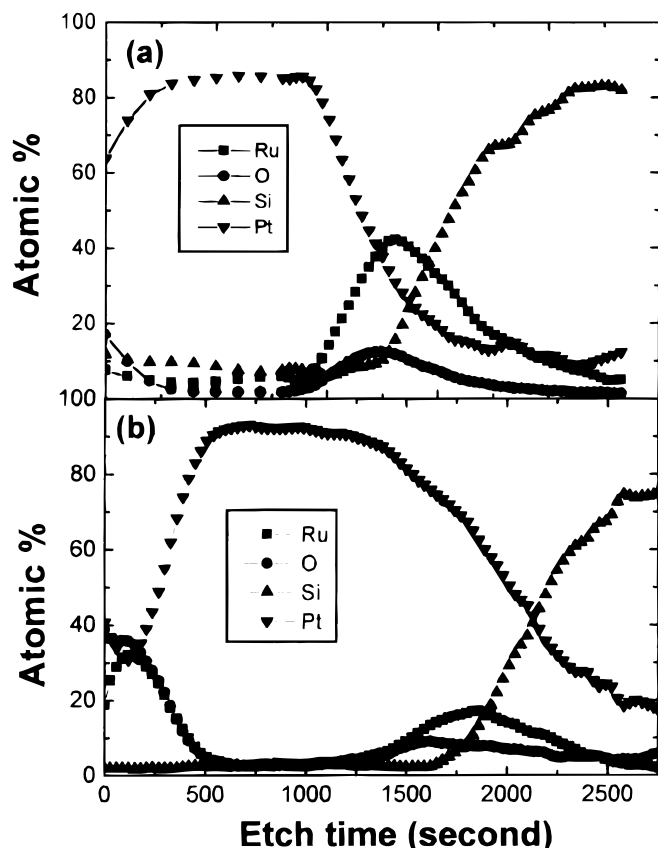


Figure 3. AES depth-profile of (a) Pt/MOCVD (RuO_2/Ru)/poly-Si and (b) Pt/dc sputtered (RuO_2/Ru)/poly-Si structures annealed at 700°C in O_2 ambient.

were expected to prevent the formation of hillocks and the intermixing of elements when they are experienced under high temperature. Figures 3a and b showed AES depth-profiles of Pt/MOCVD(RuO_2/Ru)/poly-Si and Pt/dc sputtered (RuO_2/Ru)/poly-Si structures annealed at 700°C in oxygen ambient(760 Torr), respectively. In Pt/MOCVD(RuO_2/Ru)/poly-Si structure, the dense RuO_2 deposited on Ru prevents the diffusion of Ru into the RuO_2 layer, and then an intermixing with platinum during the high temperature annealing in oxygen ambient. The diffusion of Ru into the platinum layer was not observed, and the RuO_2/Ru barrier layer seems to maintain a stable interface after annealing at 700°C . The barrier layers of RuO_2/Ru formed by MOCVD effectively prevented the interdiffusion of Pt, O, and Si. The RuO_2/Ru barrier layers also prevent the diffusion of oxygen through the Pt bottom electrode during annealing in oxygen ambient and the oxidation of poly-Si plug. On the other hand, in Pt/dc sputtered (RuO_2/Ru)/poly-Si structure, RuO_2/Ru barrier layer did not prevent the diffusion of platinum into silicon and showed an unstable interface structure. The ruthenium and oxygen exist on the platinum surface, compared with electrode structure formed by MOCVD. From this result, the second phase observed from SEM surface image might be RuO_x formed on platinum surface by the reaction of ruthenium and oxygen.

The I-V curves of as-deposited and annealed contacts at various temperatures for 1 h in oxygen ambient for Pt/MOCVD (RuO_2/Ru)/poly-Si structures become linear, which is indicative of Ohmic characteristics independent of annealing temperature after annealing at various temperatures. However, the I-V characteristics for Pt/dc-sputtered (RuO_2/Ru)/poly-Si structure cannot be measured because of high contact resistance. While the I-V characteristics are useful for examining changes in contact behavior with annealing temperature, measuring the specific contact resistance (ρ_c) gives more quantitative information. The specific contact resistivity of electrode structures as

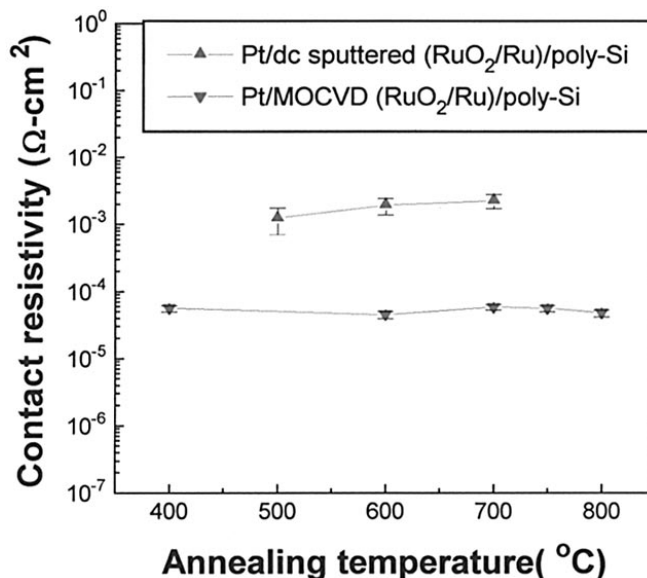


Figure 4. Specific contact resistivities of electrode structures as a function of annealing temperature.

a function of annealing temperature is shown in Fig. 4. The contact resistivity of Pt/MOCVD (RuO_2/Ru)/poly-Si structure with increasing annealing temperature almost did not vary, compared with that of as-deposited electrode structure. On the other hand, the contact resistivities of Pt/dc-sputtered (RuO_2/Ru)/poly-Si structure slightly increase with increasing annealing temperature. The contact resistivity of as-deposited electrode structure could not measure because of adhesion problem between layers. The contact resistivities of Pt/MOCVD (RuO_2/Ru)/Poly-Si and Pt/dc-sputtered (RuO_2/Ru)/poly-Si structure were about 5.0×10^{-5} and $2.0 \times 10^{-3} \Omega \text{ cm}^2$, respectively.

Conclusions

The barrier layers of RuO_2/Ru in Pt/ RuO_2/Ru stack structures formed on polycrystalline silicon by MOCVD and dc sputtering were suggested as electrode structures for integration of high dielectric materials. The barrier layers of RuO_2/Ru deposited by MOCVD showed a stable interface and did not affect the surface morphology of the platinum bottom electrode at high annealing temperature, compared with those of dc sputtering. The barrier layers formed by MOCVD effectively prevented the interdiffusion of Pt, O, and Si even at sufficiently high annealing temperature in oxygen ambient. Contacts in Pt/MOCVD (RuO_2/Ru)/poly-Si and Pt/dc sputtered (RuO_2/Ru)/poly-Si structure have a specific contact resistance of 5.0×10^{-5} and $2.0 \times 10^{-3} \Omega \text{ cm}^2$, respectively. The electrode structures of Pt/ RuO_2/Ru prepared on polycrystalline silicon by MOCVD were attractive for the integration of high dielectric capacitors.

Dr. Yoon assisted in meeting the publication costs of this article.

References

- S. G. Yoon, J. C. Lee, and A. Safari, *J. Appl. Phys.*, **76**, 2999 (1994).
- S. G. Yoon and A. Safari, *Thin Solid Films*, **254**, 211 (1995).
- W. J. Lee, S. G. Yoon, and H. G. Kim, *J. Appl. Phys.*, **80**, 5891 (1996).
- S. Yamamichi, P.-Y. Lesaichere, H. Yamaguchi, K. Takemura, S. Sone, H. Yabuta, K. Sato, T. Tamura, K. Nakajima, S. Ohnishi, K. Tokashiki, Y. Hayashi, Y. Kato, Y. Miyasaka, M. Yoshida, and H. Ono, *Tech. Dig. Int. Electron Devices Meet.*, 119 (1995).
- A. Yuuki, M. Yamamuka, T. Makita, T. Horikawa, T. Shibano, N. Hirano, H. Maeda, N. Mikami, K. Ono, H. Ogata, and H. Abe, *Tech. Dig. Int. Electron Devices Meet.*, 115 (1995).
- P. Y. Lesaichere, H. Yamaguchi, Y. Miyasaka, H. Watanabe, H. Ono, and M. Yoshida, *Integr. Ferroelectrics*, **8**, 201 (1995).
- B. D. Cullity, *Elements of X-Ray Diffraction*, 2nd ed., Addison-Wesley Pub. Co., Reading, MA (1977).
- A. Taylor, *X-Ray Metallography*, Wiley, New York (1961).
- D. K. Schroder, *Semiconductor Material and Device Characterization*, p. 114, John Wiley & Sons, Inc. New York (1990).